



Positron annihilation in B-doped and undoped single and polycrystalline Ni₃Al alloys

Wen Deng^{a,*}, Y.Y. Huang^a, R.S. Brusa^b, G.P. Karwasz^b, A. Zecca^b

^a Department of Physics, Guangxi University, 530004 Nanning, PR China

^b Istituto Nazionale per la Fisica della Materia, Dipartimento di Fisica, Università di Trento, 38050 Povo, Italy

Received 13 August 2005; received in revised form 3 November 2005; accepted 8 November 2005

Abstract

Coincidence Doppler broadening spectra measurements on B-doped and undoped single and polycrystalline Ni₃Al alloys exhibit characteristic differences. The probability of the positron–3d electron annihilations decreases with the increase of B concentration in single crystals of Ni₃Al alloys, while it increases with B concentration in polycrystals of Ni₃Al alloys, as long as the concentration of B is less than its solubility limit. The behavior of positrons and B atoms in single and polycrystals of Ni₃Al alloys has been discussed.

© 2005 Elsevier B.V. All rights reserved.

Keywords: Ni₃Al alloys; 3d Electrons; Positron annihilation

1. Introduction

Ni₃Al alloy has attractive properties for structural applications at elevated temperature. It has been recognized that single crystal of Ni₃Al is ductile but its polycrystalline form is extremely brittle. This brittleness precludes its fabrication into useful structural components [1].

Considerable effort has been made to increase the grain-boundary cohesion and to develop the alloy with sufficient ductility. The dramatic increase in ductility of polycrystalline Ni₃Al obtained by B doping was first reported by Aoki and Izumi [2] and later confirmed by several investigators [3,4]. The positive effect of B on the ductility of Ni₃Al occurs over a wide range of B concentrations, as long as the concentration of B is less than its solubility limit (about 1.5 at.%). Usmar and Lynn [5] suggested that B acts to disorder grain boundaries in hypostoichiometric Ni₃Al alloys, consequently making them more susceptible to slip and making the alloy more ductile. Heredia and Pope [6] showed that B additions improve the ductility of both single and polycrystalline Ni₃Al alloys. In order to understand the behavior of B atoms in single and polycrystalline Ni₃Al alloys more experimental evidence is needed.

Positron annihilation techniques (lifetime and Doppler broadening) are well established to detect open volume and negatively charged centers in solids [7,8]. The Doppler broadening spectrum presents information about the one-dimensional momentum distribution of the annihilating positron–electron pair [9]. In particular, the high resolution two-detector coincidence system of the Doppler broadening of positron annihilation radiation allows reducing the background of the spectrum and pointing out the contribution of positron annihilation due to core electrons that are fingerprints of the atoms [10–12].

In this work, coincidence Doppler broadening spectra of single crystals of Si, Al, Ni, polycrystal of B, single and polycrystalline Ni₃Al alloys with B concentrations from 0.00 to 1.37 at.% have been measured. The aim of this work is to study the positron annihilation sites in the alloy as well as the behavior of B atoms in single and polycrystalline Ni₃Al alloys.

2. Experimental

The samples were prepared by means of the following procedures: polycrystals of Ni₃Al with different B concentrations were separately melted in a vacuum induction furnace and cast as rods, 12 mm in diameter. The single crystalline bars were manufactured by the Bridgman technique using a seed crystal and withdrawal rate of 12 cm/h. All alloys were homogenized at 1200 °C for 4 h, cooled in the furnace to 1100 °C for 1 h and then cooled to room temperature. Both single and polycrystalline rods were cut into pieces with a thickness of 1 mm and pairs of specimens of each composition were prepared. For com-

* Corresponding author. Tel.: +86 771 3232666; fax: +86 771 3237386.
E-mail address: wdeng@gxu.edu.cn (W. Deng).

Table 1
Composition of single and polycrystalline Ni₃Al + B alloys (at.%)

Alloy no.	Ni	Al	B
1	77.11	22.89	0.00
2	75.65	23.83	0.52
3	76.30	22.33	1.37

parison, single crystals of Si, Al, Ni, polycrystal of B were also prepared. The surfaces of the specimens were then metallographically polished. After cutting and polishing, all of the specimens were annealed again at different temperatures (the single and polycrystalline Ni₃Al alloys at 650 °C, the Si, Ni, B samples at 1000 °C, the Al metal at 500 °C) for 2 h in vacuum furnace with a pressure of about 5×10^{-7} mbar, and then furnace cooled.

The chemical composition of each single crystal of Ni₃Al is the same as its polycrystalline form, as shown in Table 1. In our experiment, B concentration in the Ni₃Al alloy is less than its solubility limit in the alloy (1.5 at.%). In the following the single and polycrystalline samples corresponding to the alloy no. 1–3 will be labeled as S1–S3 and P1–P3, respectively.

Lifetime measurements have been performed in annealed single crystals of Si, Al, Ni, and polycrystal of B. The positron lifetimes in Si, Ni, Al and B are 220 ± 1 , 105 ± 1 , 160 ± 1 and 209 ± 2 ps, respectively. They are typical lifetimes of positron annihilation in defect-free samples.

Doppler broadening measurements were carried out by sandwiching a 0.6 MBq ²²Na radioactive source, supported by two kapton films, between two pieces of the same sample.

Doppler broadening spectra were measured using a two-detector coincidence system. The main detector was a high purity Ge (HPGe) detector with a resolution of 1.3 keV at 511 keV. The auxiliary detector supplying the coincidence signal was a NaI(Tl) scintillator. The NaI(Tl) detector was placed in collinear geometry with the Ge detector in order to detect the two 511 keV γ -rays from the $e^+ - e^-$ annihilation pair. With this setup, we obtain a peak to background ratio of more than 10^4 on the high-energy side of the peak. The use of the coincidence technique reduces the background remarkably on the high-energy side of the peak, while on the low energy side the effects of Compton scattering, incomplete charge collection, and 3- γ positronium decay cannot be overcome by the coincidence technique. Thus, only the high-energy side of the peak was analyzed and shown in our experiment. The coincidence spectra were taken until more than 10^7 counts had been accumulated in the peak.

The coincidence Doppler broadening spectra of single crystals of Si, Ni, Al, polycrystal of B, single and polycrystalline Ni₃Al alloys with B concentrations from 0.00 to 1.37 at.% have been measured.

3. Results and discussion

The defects in the metals or alloys can be characterized by using the usual *S* and *W* parameters, respectively [7]. The *S* parameter is defined as the ratio of the counts in the central area of the peak ($0 \leq (E_\gamma - 511 \text{ keV}) \leq 0.776 \text{ keV}$) and the total area of the peak ($0 \leq (E_\gamma - 511 \text{ keV}) \leq 9.31 \text{ keV}$). The *W* parameter is defined as the ratio of the counts in the wing area of the peak ($1.4 \text{ keV} \leq (E_\gamma - 511 \text{ keV}) \leq 9.31 \text{ keV}$) and the total area of the peak ($0 \leq (E_\gamma - 511 \text{ keV}) \leq 9.31 \text{ keV}$). The values of *W* and *S* parameters for the samples are reported in Table 2.

As it is known that the *S* parameter is an indication of defect concentration, the higher the defect concentration, the larger the *S* parameter, and vice versa. It can be seen in Table 2 that the *S* parameter of alloy no. P1 (labeled as $S(P1) = 0.4235$), is larger than that of alloy no. S1 (labeled as $S(S1) = 0.4158$), or $S(P1) > S(S1)$, this indicates that the defect concentration in the binary single crystal of Ni₃Al alloy is lower than that in the binary polycrystal of Ni₃Al alloy. In polycrystals of Ni₃Al alloys, the *S* parameters decrease with the increase of B concen-

Table 2
S and *W* parameters for the samples

Sample no.	<i>S</i>	<i>W</i>
S1	0.4158	0.3314
S2	0.4186	0.3270
S3	0.4187	0.3269
P1	0.4235	0.3219
P2	0.4192	0.3269
P3	0.4156	0.3316
Al	0.5063	0.2094
B	0.4679	0.2536
Ni	0.4174	0.3317

The error on *S* and *W* is 2×10^{-4} .

tration, this can be due to B atoms have a strong tendency to segregate to the grain boundaries, thus reduce the positron trapping rate by these defects. In single crystals of Ni₃Al alloys, the *S* parameters increase with B concentration. In order to explain these findings, it is necessary to analyze the coincidence Doppler broadening spectra.

The 511 keV annihilation line is Doppler broadened ΔE ($\Delta E = E - m_0c^2$) due to the longitudinal momentum p_L component of the annihilating positron–electron pair, where c is the light velocity, m_0 is the static mass of electron, E is gamma energy. In a Doppler experiment the longitudinal momentum component p_L in the direction of the detector is measured. The momentum component p_L is correlated to the Doppler shift ΔE by the formula $p_L = 2\Delta E/c$.

To observe the differences among different spectra, we have followed the idea introduced in [13,14] by constructing ratio curves, i.e. every spectrum is divided by a spectrum of a material chosen as reference. As a reference specimen Cz–Si p(1 0 0) was chosen in this work. Before the ratio is taken, all of the spectra have been normalized to a total area of 10^6 from 511 to 530 keV (p_L from 0 to $74.3 \times 10^{-3} m_0c$) and a smoothing routine on nine points was applied.

Fig. 1 shows the ratio curves for the Ni, Al, B elements and S1 alloy.

Fig. 2(a) shows the ratio curves for S1 and S2 alloy. The ratio curve for S3 alloy is slightly lower than that for S2 alloy, and is not shown in the figure for clarity.

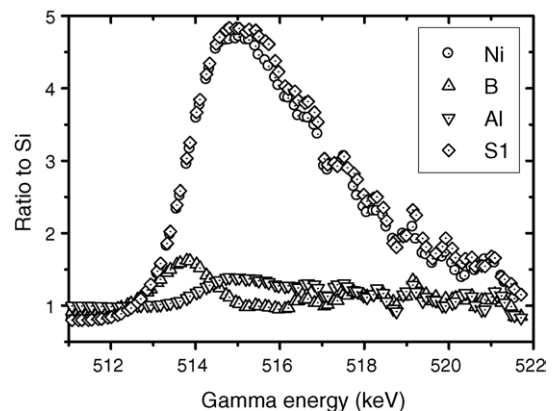


Fig. 1. Ratio curves for Ni, B, Al elements and S1 alloy. The reference sample is Si.

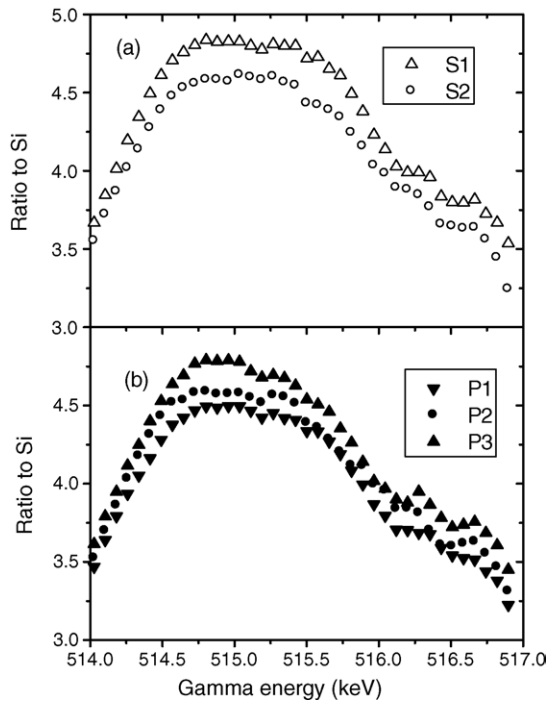


Fig. 2. (a) Ratio curves for S1 and S2 alloys. (b) Ratio curves for P1, P2, P3 alloys. The reference sample is Si.

Fig. 2(b) shows the ratio curves for P1, P2 and P3 alloy.

The shape of the ratio curves for the S and P alloys are very similar, they only differ from the height of the peak at about 515 keV. In Fig. 2(a) and (b), only the part around the maximum of the spectrum is shown for clarity.

The detailed shape of the high-momentum part of the Doppler spectrum depends on the different contribution coming from the annihilations with the electrons of each shell of the atom. Calculation of positron–electron momentum distribution on Ni metal has shown that in the $515 \text{ keV} < E_\gamma < 520 \text{ keV}$ range the dominant contribution is due to the annihilations with the 3d electrons [15]. It can be seen in Fig. 1, the peaks of the ratio curves for Ni metal and S1 alloy are at about 515 keV, and it is due to the annihilations with the 3d electrons of Ni atom.

The ratio curve for Ni metal is much higher than both Al and B curves, for both Al and B atoms without d electron, however it almost superimposes with the ratio curve for S1 alloy. This means that the annihilations with the 3d electrons of Ni atoms make the dominant contribution to the ratio curve for S1 alloy, that is, the ratio curve for S1 alloy without signal of the annihilations with the electron of Al atom. It has been known that a thermalized positron in an alloy is strongly repelled by the positive ions because of its positive charge. The positron density distribution has a “Swiss cheese” character with holes around each ion. This squeezing of the positron into interstitial regions provides a positive contribution to the ground state of energy [7]. When a positron enters the octahedral interstitial site surrounded by six Ni atoms in L_{12} ordered structure of Ni_3Al alloy, the environment of it is similar to that in Ni metal. Our experimental results indicate that the positron wave function is concentrated on the octahedral interstitial site surrounded by six

Ni atoms in L_{12} ordered structure of Ni_3Al alloy, and then annihilated with the electrons of Ni atoms. On the other hand, it can be understood by the fact that the Pauling electronegativity of Al (1.5) is smaller than that of Ni (1.8), first-principle calculation of electronic structure in Ni_3Al alloy indeed indicates that the electrons are transferred from Al to Ni [16]. This leads to the thermalized positrons drift towards the Ni sublattice in the alloy and then annihilated with the electrons of Ni atoms.

Fig. 2(a) and (b) shown that the height of the ratio curves for single crystals of Ni_3Al decreases with the increase of B concentration, while the height of the ratio curves for polycrystals of Ni_3Al increases with B concentration.

In a single crystal of Ni_3Al alloy, the defects in the alloy are mainly vacancies and dislocations, and the concentration of the defects is relatively low. The additions of B atoms into a single crystal of Ni_3Al alloy, B atoms mainly occupy the octahedral interstitial sites, decreasing the probability of positron staying in the octahedral interstitial sites, and hence the probability of the positron–3d electrons annihilations. This means that some of the positrons will annihilate with the electrons of Al atoms. Thus, the height of the peak of the ratio curve for single crystals of Ni_3Al decreases with the increase of B concentration, as shown in Fig. 2(a).

In a polycrystal of Ni_3Al alloy, the defects on grain boundaries with relatively large open volume are deep traps of positrons and B atoms [17,18]. When a positron is trapped in a defect on grain boundary of Ni_3Al alloy, the electron density and particularly the core electron density around the defect will be reduced with a consequent decrease in the probability of the positron–core electron annihilations. This will decrease the height of the peak of the ratio curve. The additions of B into a polycrystal of Ni_3Al alloy, some of B atoms segregate to the grain boundaries [3], reducing the positron trapping rate by the defects on grain boundaries, while increasing the probability of positron staying in the octahedral interstitial sites in the bulk of the alloy and hence the probability of the positron–3d electron annihilations. Thus, the height of the peak of the ratio curve for polycrystals of Ni_3Al increases with B concentration, as shown in Fig. 2(b).

The S and W parameters relate to the probability of the annihilations with the low and high momentum electrons, respectively. As the probability of the positron–high momentum electron annihilations increases, the W parameters increase, while the S parameters decrease, and vice versa. According to the above discussion, the W parameters decrease with the increase of B concentration in single crystals of Ni_3Al , while increase with B concentration in polycrystals of Ni_3Al (see Table 2).

4. Conclusions

- (1) When positrons are injected into the lattice of Ni_3Al alloy, the positron wave function is concentrated on the octahedral interstitial site surrounded by six Ni atoms in L_{12} ordered structure of Ni_3Al alloy, and then annihilated with the electrons of Ni atoms.
- (2) In a B-doped single crystal of Ni_3Al alloy, B atoms mainly occupy the octahedral interstitial sites, decreasing the prob-

ability of positron staying in the octahedral interstitial sites, and then the probability of the positron–3d electron annihilations. The probability of the positron–3d electron annihilations decreases with the increase of the concentration of B.

- (3) In a B-doped polycrystal of Ni₃Al alloy, some of B atoms segregate to the grain boundaries, reducing the positron trapping rate by the defects on grain boundaries, while increasing the probability of positron staying in the octahedral interstitial sites in the bulk of the alloy, and hence the probability of the positron–3d electron annihilations. The probability of the positron–3d electron annihilations increase with the concentration of B.

Acknowledgments

This work was supported by the National Natural Science Foundations of China under Grant No. 50161001, Guangxi University Key Program for Science and Technology under Grant No. 2003ZD04, and the Ministero della Università e della Ricerca Scientifica e Tecnologica. One of the authors (Wen Deng) thanks ICTP Program for Training and Research in Italian Laboratories.

References

- [1] C.T. Liu, D.P. Pope, in: J.H. Westbrook, R.L. Fleisher (Eds.), *Intermetallic Compounds: Principles and Practice*, 2, John Wiley, 1995, p. 17.
- [2] K. Aoki, O. Izumi, *Nippon Kinzoku Gakkaishi* 43 (1979) 1190.
- [3] C.T. Liu, C.L. White, J.A. Horton, *Acta Metall.* 33 (1985) 213.
- [4] A.I. Taub, S.C. Huang, K.M. Chang, *Metall. Trans. A* 42 (1984) 399.
- [5] S.G. Usmar, K.G. Lynn, *J. Mater. Res.* 4 (1989) 55.
- [6] F.E. Heredia, D.P. Pope, *Acta Metall. Mater.* 39 (1991) 2017.
- [7] R.N. West, *Adv. Phys.* 22 (1973) 263.
- [8] S. Gialanella, R.S. Brusa, W. Deng, F. Marino, T. Spataru, G. Principi, *J. Alloys Compd.* 317 (2001) 485.
- [9] K.G. Lynn, J.R. MacDonald, R.A. Boie, L.C. Feldman, J.D. Gabbe, E. Bonderup, J. Golochenko, *Phys. Rev. Lett.* 38 (1977) 241.
- [10] M. Alatalo, H. Kauppinen, K. Saarinen, M.J. Puska, J. Mäinen, P. Hautajävi, R.M. Nieminen, *Phys. Rev. B* 51 (1995) 4176.
- [11] S. Szpala, P. Asoka-Kumar, B. Nielsen, J.P. Peng, S. Hayakawa, K.G. Lynn, H.J. Gossmann, *Phys. Rev. B* 54 (1996) 4722.
- [12] R.S. Brusa, W. Deng, G.P. Karwasz, A. Zecca, D. Pliszka, *Appl. Phys. Lett.* 79 (2001) 1492.
- [13] R.S. Brusa, W. Deng, G.P. Karwasz, A. Zecca, *Nucl. Instrum. Meth. Sec. B* 194 (2002) 519.
- [14] W. Deng, Y.Y. Huang, R.S. Brusa, G.P. Karwasz, A. Zecca, *J. Alloys Compd.* 386 (2005) 103.
- [15] V.J. Ghosh, M. Alatalo, P. Asoka-Kumar, B. Nielsen, K.G. Lynn, *Phys. Rev. B* 61 (2000) 10092.
- [16] D. Hackenbracht, J. Küler, *J. Phys. F: Met. Phys.* 10 (1980) 427.
- [17] V. Vitek, J.J. Kruisman, J.Th.M. De Hosson, in: M.H. Yoo, W.A.T. Clark, C.L. Briant (Eds.), *Proceedings of the MRS Symposium on Interfacial Structure, Properties and Design*, Reno, Nevada, 1988, p. 139.
- [18] W. Deng, L.Y. Xiong, S.H. Wang, J.T. Guo, C.W. Lung, *J. Mater. Sci. Lett.* 13 (1994) 313.